TITLE:

Design and Implementation of a Bespoke Robotic Manipulator for Extra-corporeal Ultrasound

AUTHORS AND AFFILIATIONS:

Shuangyi Wang[1*], James Housden[1*], Yohan Noh[1], Anisha Singh[2], Junghwan Back[3], Lukas Lindenroth[3], Hongbin Liu[3], Joseph Hajnal[1], Kaspar Althoefer[4], Davinder Singh[2], Kawal Rhode[1]

[1]School of Biomedical Engineering & Imaging Sciences, King's College London, UK
[2]Xtronics Ltd., Gravesend, UK
[3]Department of Informatics, King's College London, UK
[4]Faculty of Science & Engineering, Queen Mary University of London, UK
∗ Both authors contributed equally to this manuscript.

Corresponding Author:
Shuangyi Wang
shuangyi.wang@kcl.ac.uk
Tel: +44 (0) 7835234417

Email Addresses of Co-authors:
James Housden (richard.housden@kcl.ac.uk)
Yohan Noh (yohan.noh@kcl.ac.uk)
Anisha Singh (lucky@xtronics.co.uk)
Junghwan Back (junghwan.back@kcl.ac.uk)
Lukas Lindenroth (lukas.lindenroth@kcl.ac.uk)
Hongbin Liu (hongbin.liu@kcl.ac.uk)
Joseph Hajnal (jo.hajnal@kcl.ac.uk)
Kaspar Althoefer (k.althoefer@qmul.ac.uk)
Davinder Singh (xtronics@me.com)
Kawal Rhode (kawal.rhode@kcl.ac.uk)

KEYWORDS:
Medical robot, robotic ultrasound, extra-corporeal ultrasound, robot design, mechanism design, linkages and manipulators, robot safety, 3D-printing, rapid prototyping.

SUMMARY:

This paper introduces the design and implementation of a bespoke robotic manipulator for extra-corporeal ultrasound examination. The system has five degrees-of-freedom with lightweight joints made by 3D printing and a mechanical clutch for safety management.

ABSTRACT:

With the potential for high precision, dexterity, and repeatability, a self-tracked robotic system

---

can be employed to assist the acquisition of real-time ultrasound. However, limited numbers of robots designed for extra-corporeal ultrasound have been successfully translated into clinical use. In our study, we aim to build a bespoke robotic manipulator for extra-corporeal ultrasound examination, which is lightweight and has a small footprint. The robot is formed of five specially-shaped links and custom-made joint mechanisms for probe manipulation to cover the necessary range of motion with redundant degrees-of-freedom to ensure patient safety. The mechanical safety is emphasized with a clutch mechanism to limit the force applied to patients. As a result of the design, the total weight of the manipulator is less than 2 kg and the length of the manipulator is about 25 cm. The design has been implemented, and simulation, phantom and volunteer studies performed, to validate the range of motion, ability to make fine adjustments, mechanical reliability, and safe operation of the clutch. This paper details the design and implementation of the bespoke robotic ultrasound manipulator with the design and assembly methods illustrated. Testing results to demonstrate the design features and clinical experience of using the system are presented. It is concluded that the current proposed robotic manipulator meets the requirements as a bespoke system for extra-corporeal ultrasound examination and has great potential to be translated into clinical use.

INTRODUCTION:

An extra-corporeal robotic ultrasound (US) system refers to the configuration in which a robotic system is utilized to hold and manipulate an US probe for external examinations, including use in cardiac, vascular, obstetric, and general abdominal imaging[1]. The use of such a robotic system is motivated by the challenges of manually holding and manipulating a US probe: e.g. the challenge of finding standard US views required by clinical imaging protocols and the risk of repetitive strain injury[2-4], and also by the needs of US screening programs: e.g. the requirement for experienced sonographers to be on-site[5,6]. With emphases on different functionalities and target anatomies, several robotic US systems, as reviewed in the works[1,7,8], have been introduced since the 1990s to improve different aspects of US examination: e.g. long-distance tele-operation[9-12], as well as robot-operator interaction and automatic control[13,14]. In addition to the robotic US systems used for diagnostic purpose, robotic high intensity focused ultrasound (HIFU) systems for treatment purposes have been widely investigated as summarized in[1], with some of the recent works such as[15,16] reported for the latest progress.

Although several robotic US systems have been developed with relatively reliable technologies for control and clinical operation, only a few of them have been successfully translated into clinical use, such as the commercially-available system from[17]. One possible reason is the low level of acceptance for large-size industrial-looking robots working in a clinical environment, from the point of view of both patients and sonographers. Additionally, for safety management, the majority of the existing US robots rely on force sensors to monitor and control the applied pressure to the US probe, while more fundamental mechanical safety mechanisms to limit the force passively are usually not available. This may also cause concerns when translating into clinical use as the safety of robot operation would be purely dependent on electrical systems and software logic.

With the recent advancements of 3D printing techniques, specially-shaped plastic links with custom-made joint mechanisms could provide a new opportunity for developing bespoke medical robots. Carefully designed lightweight components with a compact appearance could improve the clinical acceptance. Specifically for US examination, a bespoke medical robot aimed to be translated into clinical use should be compact, with enough degrees-of-freedom (DOFs) and range of motion to cover the region of interest of a scan; for example, the abdominal surface including both the top and sides of the belly. Additionally, the robot should also incorporate the ability to do fine adjustments of the US probe in a local area, when trying to optimize an US view. This usually includes tilting movements of the probe within a certain range as suggested in[18,19]. To further address the safety concerns, it is expected that the system should have passive mechanical safety features which are independent of electrical systems and software logic.

In this paper, we present the detailed design and assembly method of a 5-DOF dexterous robotic manipulator, which is used as the key component of an extra-corporeal robotic US system. The manipulator consists of several lightweight 3D-printable links, custom-made joint mechanisms, and a built-in safety clutch. The specific arrangement of DOFs provides full flexibility for probe adjustments, allowing easy and safe operation in a small area without colliding with the patient. The proposed multi-DOF manipulator aims to work as the main component that is in contact with patients and it can be simply attached to any conventional 3-DOF global positioning mechanism to form a complete US robot with fully active DOFs to perform an US scan.

PROTOCOL:

1. Print all the links (L_0, L_1, L_2, L_3, and L_4) and the end-effector as shown in **Figure 1** with ABS (acrylonitrile butadiene styrene) plastic, PLA (polylactic Acid) plastic, or Nylon using a 3D printing service. Use the STL files provided in the supplementary materials when printing.

Note: changes in shape and scale of each part can be made based on the provided files. The inner profile of the end-effector can be changed to fit different US probes.

2. Print all the required additional components as shown in **Figure 2** in Nylon using a 3D printing service. Refer to the material list for the required number of each component. Use the STL files provided in the supplementary materials when printing.

3. Polish all the printed plastic parts with polishing tools if necessary. Remove supporting materials left from 3D printing if necessary.

Note: some structures in the provided end-effector design are for a force sensor, which is not a part of the current reported protocol and will not be used for the assembly. The force sensor design concept has been reported in previous work[20], thus it is not covered in this paper.

3. Assembly of Joint 1 (J_1) based on **Figure 3**:

3.1. Place the four small geared stepper motors (with 20-teeth spur gears attached) into the mounting cavities of L_0 and mount them with screws.

3.2. Place the two 37 mm O.D bearings into the bearing housings of L_0 and secure the 120-teeth spur gear (Type A) onto the hexagon key of L_1.

3.3. Insert the shaft on L_1 into the shaft hole on L_0 with the four small driving spur gears and the large driven spur gear engaged and assemble the shaft collar to secure and retain the shaft.

4. Assembly of Joint 2 (J_2) based on **Figure 4**:

4.1 Place the four small geared stepper motors (with 20-teeth spur gears attached) into the mounting cavities of L_1 and mount them with screws.

4.2. Attach the two 120-teeth spur gears (Type B) to the two 37 mm O.D bearings and position them into the gear cavities of L_1, with the 120-teeth spur gear (Type B) engaged with the 20-teeth spur gears mounted on the motors.

4.3. Insert the four ball-spring pairs into the clutch holes in L_2 with the two round clutch covers pushing the spring into the clutch mechanism for pre-loading.

4.4. Insert the shaft (e.g. an M6 bolt with a nut) into the bores of L_1 and L_2 with the two joints properly aligned and place the two 12 mm O.D bearings into the bearing housings of L_2.

5. Assembly of Joint 3 (J_3) based on **Figure 5**:

5.1. Place the two small geared stepper motors (with 20-teeth spur gears attached) into the mounting cavities of L_2 and mount them with screws.

5.2. Place the 37 mm O.D bearing into the bearing housing of the 120-teeth spur gear (Type C) and place the 32 mm O.D bearing into the bearing housing of L_3.

5.3. Secure the large spur gear into the hexagon keyhole of L_3 (additional screws can be used if necessary) and insert the shaft on L_2 into the bores on the large spur gear and L_3, with the small and the large spur gears engaged. Ensure the driven large spur gear rotates freely on the 37 mm O.D bearing and L_3 rotates freely on the 32 mm O.D bearing.

6. Assembly of Joint 4 (J_4) based on **Figure 6**:

6.1. Place the two small geared stepper motors into the mounting cavities of L_3 and mount them with screws. Place the 8 mm O.D bearings into the bearing housings of L_4.

6.2. Mount the 20-teeth long spur gear onto the two small stepper motors and insert the shaft into the shaft hole of L_3 and L_4 after the two links are aligned (e.g. using an M5 bolt with a nut). Ensure the built-in driven gear structure on L_4 mates with the 20-teeth long spur gear.

7. Assembly of Joint 5 (J_5) based on **Figure 7**:

7.1. Place the two small geared stepper motors (with 18-teeth bevel gears attached) into the mounting cavities of L_4 and mount them with screws.

7.2. Position the driving 144-teeth bevel gear onto the extrusion of L_4 with its bottom gear part engaged with the two driving small bevel gears.

7.3. Insert the end-effector into the keyway of the large bevel gear and vertically position the end-effector with the end-effector collar screwed onto it. Ensure the end-effector collar, rotating on the top round surface of $L_{4,}$ holds and positions the end-effector vertically.

REPRESENTATIVE RESULTS:

Following the protocol, the resulting system is a robotic manipulator with five specially-shaped links (L_0 to L_4) and five revolute joints (J_1 to J_5) for moving, holding and locally tilting an US probe (**Figure 8**). The top rotation joint (J_1), with gear mechanisms actuated by four motors, can rotate the following structures 360 degrees to allow the US probe to point towards different sides of the scanning area, such as the top, bottom, and sides of the abdomen. The main tilting joint (J_2), with gear mechanisms actuated by four motors, is used to tilt down the probe to align with the surface of the scanning area. As this joint is also crucial to the force management, a mechanical clutch with balls, springs, and detent holes was incorporated. The last three orthogonal revolute joints (J_3, J_4, and J_5), with gear mechanisms actuated by two motors each, are used to control the tilting and axial rotation of the probe, allowing fine adjustments of the probe in a local area. The last revolute joint J_5 also allows the mounting of an US probe in a specially-shaped end-effector. The total weight and length of the proposed robotic manipulator, which is the only structure usually on top of the patient’s body, are less than 2 kg and 25 cm. The resulting design is such that a large range of probe positions can be reached with only small movements of the remaining global positioning mechanism when using the proposed robotic US manipulator. Considering just the proposed manipulator on its own, the probe can be rotated axially to any angle, tilted to follow a surface angled between 0 and 110 degrees to the horizontal in any direction, and positioned within a circle of diameter 360 mm. Additionally, the revolute joints J_3 and J_4 provide a tilting angle in the range -180 to 180 degrees and -30 to 45 degrees, respectively in two directions, which is used for local fine adjustments of the US probe. The ranges of movements and tilting angles meet the required ranges for obtaining an ideal acoustic window for US examinations as suggested in[18,19]. The technical details of the proposed robotic manipulator are summarized in Table 1 (Denavit–Hartenberg parameters and joint specifications) based on the coordinate definitions shown in **Figure 8**. The estimated cost of the system is 500 GBP based on the current manufacturing method, components and materials.

As an example used in this research, we employed a global positioning system which has a revolute joint (R_1) with a chain mechanism for rotating the complete arm and a two-bar arm-based set of parallel link mechanisms (R_2 and R_3) with worm-gear drives (**Figure 9**). This 3-DOFs mechanism will work with the proposed 5-DOF manipulator to form a complete robotic US system. Based on the proposed robotic manipulator and the example global positioning option used for this research, **Figure 10** shows a simulation example of the robot in positions around an abdominal phantom, demonstrating that it is able to reach around both sides of the abdomen and a range of positions on top. The design of the redundant joints in the system, particularly the configurations of J_1 and J_2, allows tilting the probe to large angles with most of the mechanical structures still staying away from the patient's body, as can be observed from **Figure 10**. Consequently, with the last three joints (J_3, J_4, and J_5) specified to rotate within limited ranges for fine tilting adjustments, collision is avoided between the moving parts of the robot and the patient's body.

With the electronics and the conventional stepper motor control system developed, experiments have been performed to test the output force and validate the expected range of motion. The current control unit is a box with microcontrollers, stepper motor drivers, power supply and regulators, and other supporting electronic components included. The overall size of the control box is 40 cm long, 23 cm wide and 12 cm deep. Based on the repeated testing of the system, the maximum force that the robotic manipulator can currently exert is set to 27 N before the mechanical safety clutch is triggered, specifying the output force range of the proposed system to be 0 N to 27 N. With the configuration of the mechanical clutch, it was verified by repeated testing that in the default position when the clutch is engaged, the balls are partially in the detent holes of L_1. Therefore the movements of the driven large spur gears actuate L_2. However, when excessive force is exerted at the end-effector, the clutch is disengaged with the balls moving out of the detent holes of L_1.

The range of motion of each joint reported in Table 1 was also repeatedly tested and validated. The reliable working of the robotic manipulator over a long period of time has been extensively tested on a fetal phantom and continuously verified with abdominal scans of internal healthy volunteers (**Figure 11**). The study was approved by the local ethics committee. So far, 20 volunteer scans for general abdominal ultrasound examinations using the robotic manipulator have been successfully performed with basic software control of the robot, mainly to evaluate the reliability and feasibility of the mechanical design. It was concluded from the phantom and volunteers studies that the current design of the robotic manipulator can reach the required movement range at the required force, and provides enough fine adjustment, to obtain images similar to the hand-held operation of the US probe for abdominal imaging. For all these scans, no safety concerns or uncomfortable feelings were reported by the volunteers. The selection of motors, mechanical ratios of mechanisms, and power levels, have been verified such that they ensure the reliable movement of the probe on the patient's body, while at the same time resulting in slippage if excessed forces are generated. Further details of this on-going volunteer study and clinical evidence for the use of the robot will be presented separately.

FIGURE AND TABLE LEGENDS:

Figure 1: CAD drawing of all the links (L_0, L_1, L_2, L_3, and L_4) and the end-effector. The shape of each link is shown for reference when 3D printing using the provided STL files. The end-effector is illustrated with an US probe included in the assembly.

Figure 2: CAD drawing of the required additional components. The shape of each component is shown for reference when 3D printing using the provided STL files. The components include spur and bevel gears in different sizes, shaft collar, clutch cover, and end-effector collar.

Figure 3: Assembly instruction for J_1. The required links, motors, gears, and bearings are shown with some structures changed to transparent to illustrate the assembly.

Figure 4: Assembly instruction for J_2. The required links, motors, gears, ball-spring pairs, and bearings are shown with some structures changed to transparent to illustrate the assembly.

Figure 5: Assembly instruction for J_3. The required links, motors, gears, and bearings are shown with two perspective views to illustrate the assembly.

Figure 6: Assembly instruction for J_4. The required links, motors, gears, and bearings are shown with the assembled J_4 mechanism indicated.

Figure 7: Assembly instruction for J_5. The required link and end-effector, motors, and gears are shown with some structures changed to transparent to illustrate the assembly.

Figure 8: **Summary of the proposed 5-DOF robotic manipulator with the end-effector holding an US probe.** The coordinate definition of each joint and the overall size of the assembled manipulator are indicated.

Figure 9: CAD drawing of the example global positioning device. This arm-based device is used to work with the proposed robotic manipulator for testing. The notations and the main dimensions are shown in the drawing.

Figure 10: Kinematic simulation of four different scanning postures around the phantom. This demonstrates an adequate range of motion for a typical abdominal US scan.

Figure 11: Implemented US robot using the described protocol. (a) The robotic manipulator with the example global positioning mechanism; (b) clinical use of the proposed robotic manipulator on a patient's abdominal area.

Table 1: Technical details of the proposed robotic manipulator, including the Denavit–Hartenberg parameters and the joint specifications.

DISCUSSION:

Unlike many other industrial robots that have been translated into medical applications, the proposed robotic manipulator described in the protocol was specifically designed for US examinations according to the clinical requirements for the range of motion, application of force, and safety management. The lightweight robotic manipulator itself has a wide range of movements sufficient for most extra-corporeal US scanning without the need for large movements of the global positioning mechanism. As the closest mechanical structure to the patient, the proposed links are also specially-shaped to be away from the patient. With most DOFs embedded into a compact manipulator, robotic US scanning using this device can be done in an intuitive way similar to human operation without the necessity of occupying a large space. Because of all these features, we expect the system produced following the protocol could gain acceptance from the clinicians and patients, which is being validated with the on-going volunteer study. With the proposed robotic manipulator, different conventional architectures for global positioning can be used based on the particular requirement, such as a gantry or ceiling mounting designs. An example global positioning device was used in this paper to enable the tests of the proposed robotic manipulator.

The current protocol suggests that all the links can be printed using ABS or PLA plastics, or Nylon based on the availability of the local 3D printing service, while using the Nylon prints is preferred in general due to its material strength. Importantly as stated in the protocol, the additional components, especially the gears, should be printed with Nylon or other strong materials to ensure the reliability of the system. As new 3D printing materials are introduced, the use of materials could be altered. The current protocol employs an end-effector specifically designed for a particular US probe with the probe's 3D shape scanned by a CT imaging system to assist the design of the inner profile of the end-effector. When the manipulator is used with other US probes with different shapes, it is important to ensure that the inner profile of the end-effector is re-designed to tightly mate with the outer profile of the US probe, in order to guarantee the safe holding of the probe. The 3D shape and profile of the probe could also be obtained from other types of 3D scanning. Additionally, it should be noted that some of the design details described in the protocol, such as exact shapes and dimensions, shaft sizes, mounting keyways, screws, and use of bearings, could be altered. For the same reason, some of the details are not provided when it is obvious based on common knowledge of mechanical design.

The current design has a passive mechanical clutch which can be adjusted and used to limit the maximum force applied to the patient. This is a safety feature that does not rely on any electrical systems or software logic, which guarantees the fundamental safety for using the robot for US examinations. The triggering point was set based on the range from our previous measurements[21] of the vertical force applied by human operators to the patients during normal US scans as well as similar results reported from the existing literature[18], both of which suggest that the maximum vertical force usually does not exceed 20 N. This was treated as the prerequisite that the trigger force of the clutch should be more than 20 N with some given allowances. The amount of triggering force can be adjusted by changing the number of ball-spring pairs, the spring constant, the size of the detent holes, and the pre-loading of the springs[22]. A potential modification of the designed protocol for this is to change the numbers of cavities for holding the ball-spring pairs in L_2. In practice when using the proposed system, the correct working of the clutch can be easily verified by manually rotating the clutch joint and having the clutch disengage and re-engage before any robotic US examination is performed. In the current protocol, the safety clutch is only applied to J_2 as this joint is designed to align the probe with the surface of the abdomen and can be directly used to limit the vertical force exerted on the patient by the US probe. With a similar concept, a safety clutch can also be implemented for the J_1 spur gear, which will ensure the safety of the J_1 rotational movement of the following structures. This is not seen as an essential safety feature in the current protocol, but could be a potential modification for a finalized version. The last three joints J_3, J_4, and J_5 are used for fine adjustments of the probe's orientation. Kinematically, they are not used to generate any excessive force and are not likely to collide with any obstacle. To minimize the size and weight of the proposed manipulator, a safety mechanical clutch is not suggested for these three joints in any modification of the protocol.

Following the proposed protocol to build the proposed manipulator for US examinations, the same reliability of the mechanical system, the same ranges of motion, similar weights of the whole manipulator, and a similar level of triggering force of the clutch are expected as are reported in this paper. However, the repeatability and accuracy of the movements, as well as the repeatability of the exact triggering force level of the mechanical clutch, would strongly depend on the 3D-printing and assembly accuracy compared to the CAD design. This cannot be guaranteed for the current prototype as a lab-based low-end 3D printing service was used for manufacturing and the assembly was done manually for the purpose of preliminary prototyping. It is expected that an industrial level of manufacturing and assembly following the design protocol would result in good repeatability and high accuracy, although this is not our currently our aim before the system is made into a final product for clinical trial. Testing of the performance would also require a separate protocol, which includes kinematic modelling, a robotic control method, motion tracking and calibration methods, and is thus not included in the current paper. Similarly, the control precision and response of the proposed manipulator are determined by the motor control method, robot control algorithm, and communication between the electronics of the manipulator and the control interface. As these are beyond the aim of the current protocol of introducing the new mechanical design and can be implemented using many existing architectures, details are not provided in this paper.

ACKNOWLEDGMENTS:

This work was supported by the Wellcome Trust IEH Award [102431] and by the Wellcome/EPSRC Centre for Medical Engineering [WT203148/Z/16/Z]. The authors acknowledge financial support from the Department of Health via the National Institute for Health Research (NIHR) comprehensive Biomedical Research Centre award to Guy's & St Thomas' NHS Foundation Trust in partnership with King's College London and King's College Hospital NHS Foundation Trust.

DISCLOSURES:

The authors have nothing to disclose.

REFERENCES:

1. Priester, A. M., Natarajan, S., Culjat, M. O. Robotic ultrasound systems in medicine. *IEEE transactions on ultrasonics, ferroelectrics, and frequency control*. **60** (3), 507-523 (2013).
2. Magnavita, N., Bevilacqua, L., Mirk, P., Fileni, A., Castellino, N. Work-related musculoskeletal complaints in sonologists. *Journal of occupational and environmental medicine*. **41** (11), 981-988 (1999).
3. Jakes, C. Sonographers and Occupational Overuse Syndrome: Cause, Effect, and Solutions.

Journal of Diagnostic Medical Sonography. **17** (6), 312-320 (2001).

4. Society of Diagnostic Medical Sonography. Industry Standards for the Prevention of Work-Related Musculoskeletal Disorders in Sonography: Consensus Conference on Work-Related Musculoskeletal Disorders in Sonography. *Journal of Diagnostic Medical Sonography*. **27** (1), 14-18 (2011).

5. LaGrone, L. N., Sadasivam, V., Kushner, A. L., Groen, R. S. A review of training opportunities for ultrasonography in low and middle income countries. *Tropical medicine & international health: TM & IH*. **17** (7), 808-819 (2012).

6. Shah, S. et al. Perceived barriers in the use of ultrasound in developing countries. *Critical ultrasound journal*. **7** (1), 28 (2015).

7. Swerdlow, D. R., Cleary, K., Wilson, E., Azizi-Koutenaei, B., Monfaredi, R. Robotic Arm–Assisted Sonography: Review of Technical Developments and Potential Clinical Applications. *American Journal of Roentgenology*. **208** (4), 733-738 (2017).

8. Nouaille, L., Laribi, M., Nelson, C., Zeghloul, S., Poisson, G. Review of Kinematics for Minimally Invasive Surgery and Tele-Echography Robots. *Journal of Medical Devices*. **11** (4), 040802 (2017).

9. Georgescu, M., Sacccomandi, A., Baudron, B., Arbeille, P. L. Remote sonography in routine clinical practice between two isolated medical centers and the university hospital using a robotic arm: a 1-year study. *Telemedicine and e-Health*. **22** (4), 276-281 (2016).

10. Arbeille, P. et al. Use of a robotic arm to perform remote abdominal telesonography. *American journal of Roentgenology*. **188** (4), W317-W322 (2007).

11. Arbeille, P. et al. Fetal tele-echography using a robotic arm and a satellite link. *Ultrasound in obstetrics & gynecology*. **26** (3), 221-226 (2005).

12. Vieyres, P. et al. A tele-operated robotic system for mobile tele-echography: The OTELO project. *M-Health*. Springer, Boston, MA. 461-473 (2006).

13. Abolmaesumi, P., Salcudean, S. E., Zhu, W.H., Sirouspour, M. R., DiMaio, S. P. Image-guided control of a robot for medical ultrasound. *IEEE Transactions on Robotics and Automation*. **18** (1), 11-23 (2002).

14. Abolmaesumi, P., Salcudean, S., Zhu, W. Visual servoing for robot-assisted diagnostic ultrasound. *Engineering in Medicine and Biology Society, Proceedings of the 22nd Annual International Conference of the IEEE*. IEEE. 2532-2535 (2000).

15. Menikou, G., Yiallouras, C., Yiannakou, M., Damianou, C. MRI-guided focused ultrasound robotic system for the treatment of bone cancer. *The International Journal of Medical Robotics and Computer Assisted Surgery*. **13** (1), e1753 (2017).

16. Yiallouras, C. et al. Three-axis MR-conditional robot for high-intensity focused ultrasound for treating prostate diseases transrectally. *Journal of therapeutic ultrasound*. **3** (1), 2 (2015).

17. Telemedecine: MELODY, a remote, robotic ultrasound solution. <*http://www.adechotech.com/products/>.* (2018).

18. Essomba, T. et al. A specific performances comparative study of two spherical robots for tele-echography application. *Proceedings of the Institution of Mechanical Engineers, Part C: Journal of Mechanical Engineering Science*. **228** (18), 3419-3429 (2014).

19. Bassit, L. A. Structure me´canique a` modules sphe´riques optimise´es pour un robot me´dical de te´le´-e´chographie mobile. *PhD thesis, Université d'Orléans*. (2005).

20. Noh, Y. et al. Multi-Axis force/torque sensor based on Simply-Supported beam and optoelectronics. *Sensors*. **16** (11), 1936 (2016).

21. Noh, Y. et al. An ergonomic handheld ultrasound probe providing contact forces and pose information. *Engineering in Medicine and Biology Society, Proceedings of the 37th Annual International Conference of the IEEE*. IEEE. 5773-5776 (2015).

22. Translational detent component with asymmetric notch geometry. <*https://www.maplesoft.com/support/help/MapleSim/view.aspx?path=DrivelineComponentLibrary/translationalDetent*>. (2018).

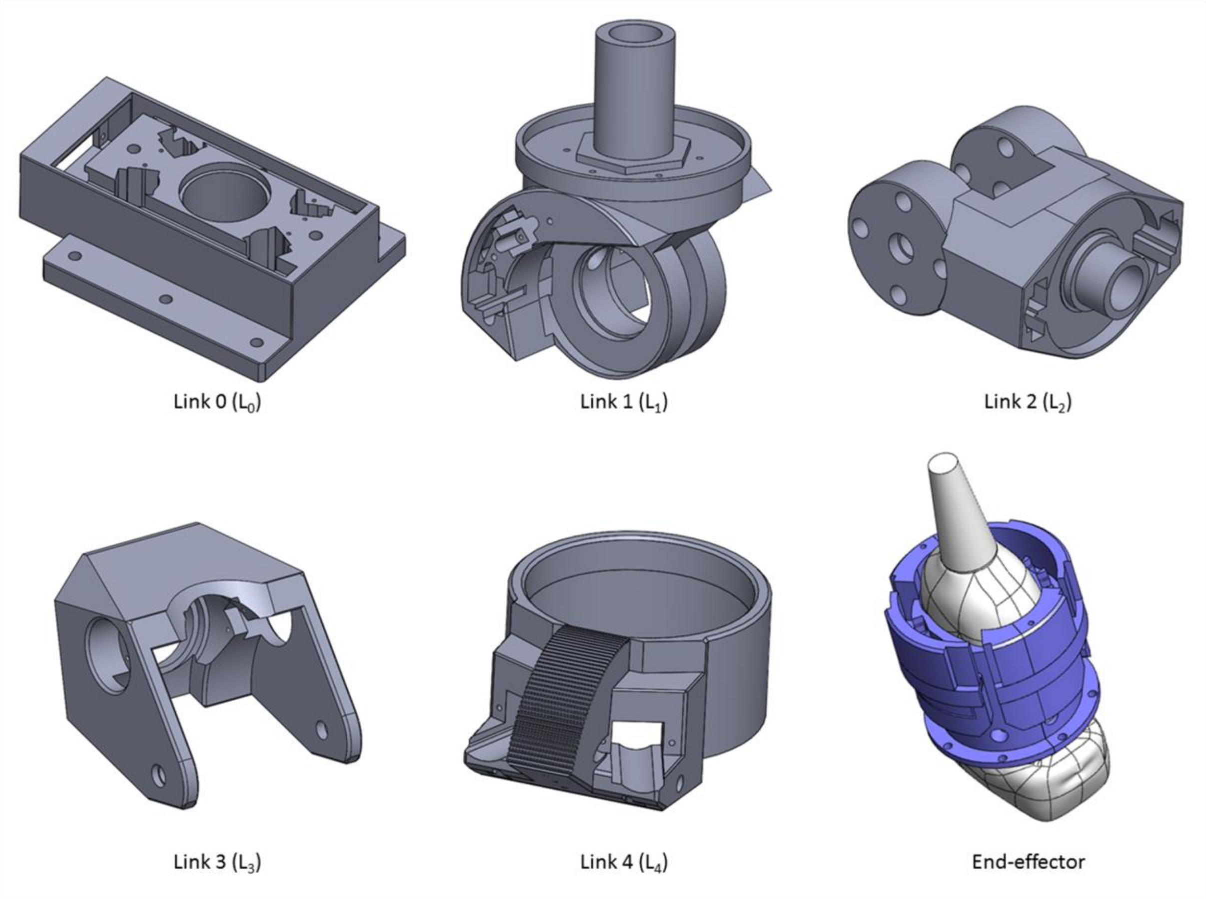

Link 0 (L_0)

Link 1 (L_1)

Link 2 (L_2)

Link 3 (L_3)

Link 4 (L_4)

End-effector

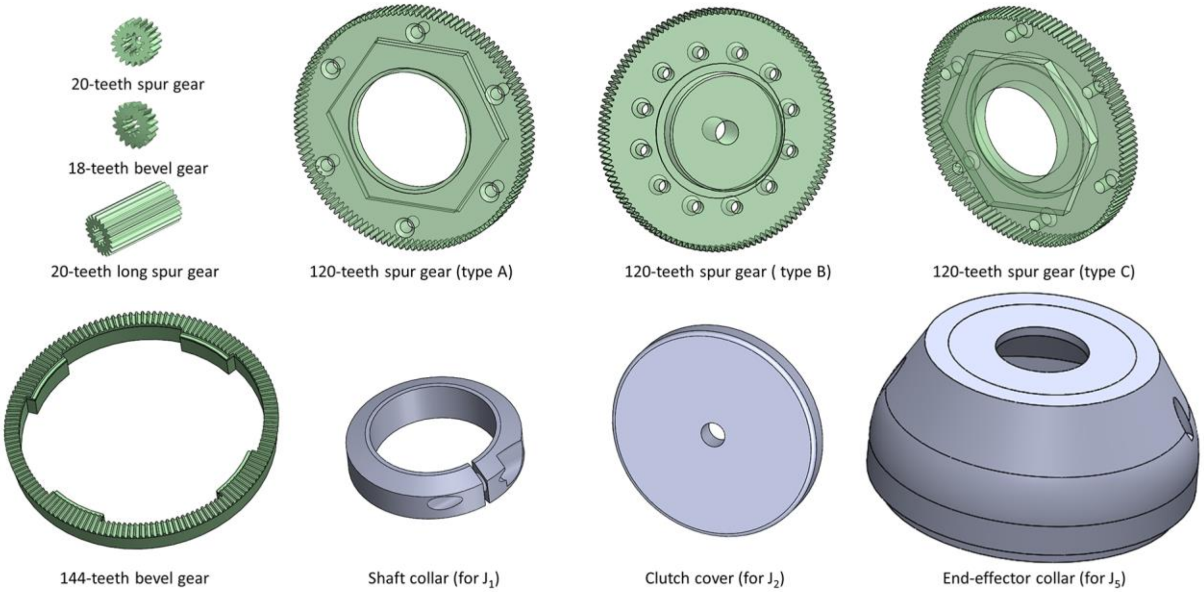

20-teeth spur gear

18-teeth bevel gear

20-teeth long spur gear

120-teeth spur gear (type A)

120-teeth spur gear (type B)

120-teeth spur gear (type C)

144-teeth bevel gear

Shaft collar (for J_1)

Clutch cover (for J_2)

End-effector collar (for J_5)

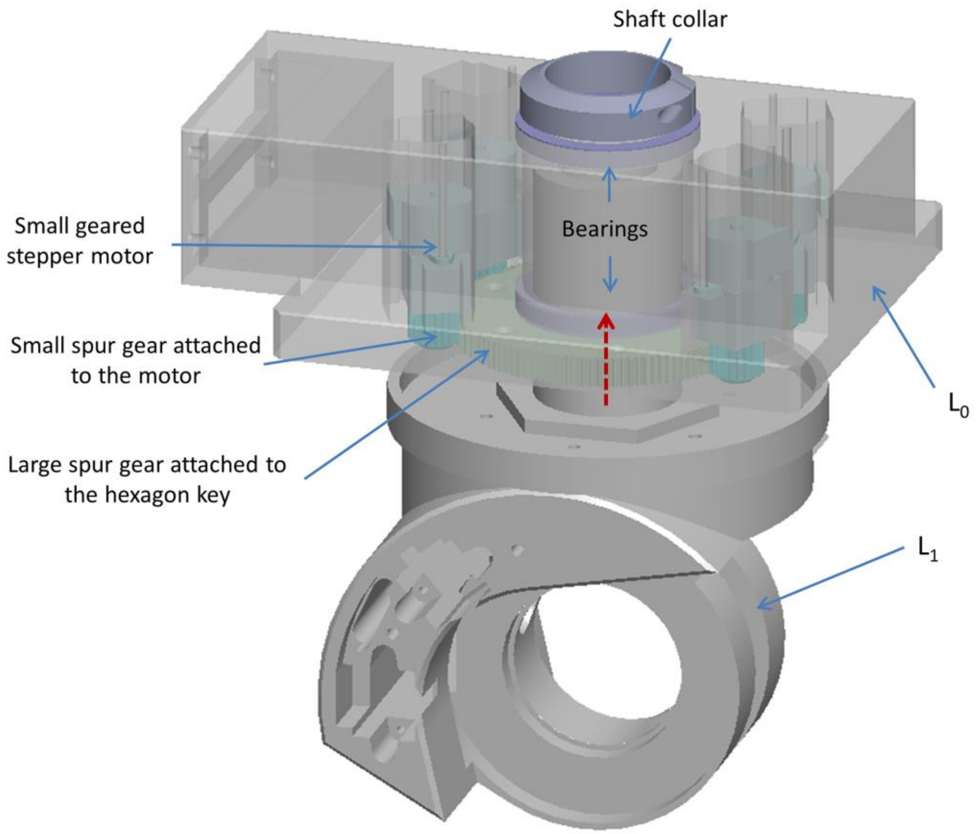
Shaft collar
Small geared stepper motor
Bearings
Small spur gear attached to the motor
Large spur gear attached to the hexagon key
L_0
L_1

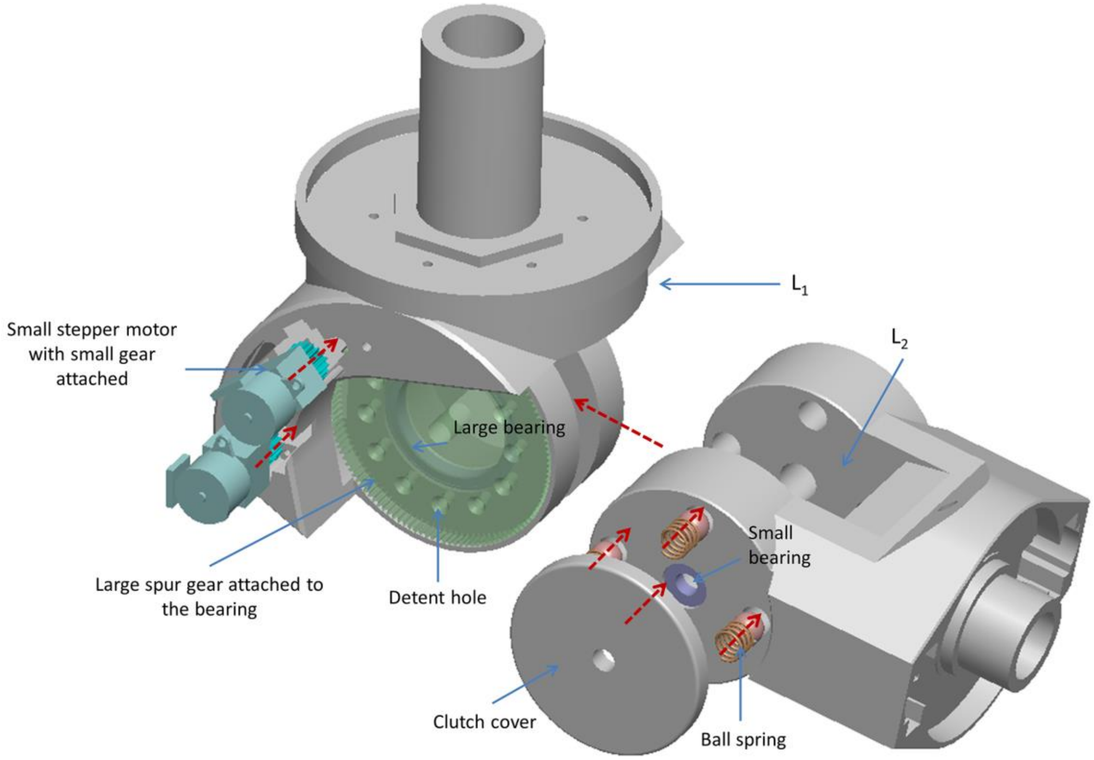
L_1
L_2
Small stepper motor with small gear attached
Large bearing
Small bearing
Large spur gear attached to the bearing
Detent hole
Clutch cover
Ball spring

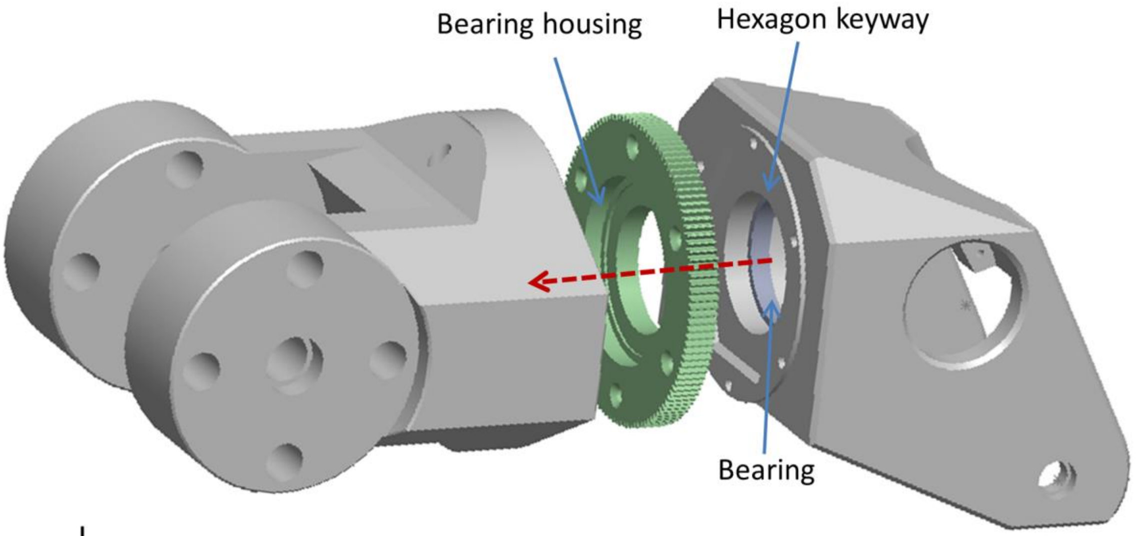
Bearing housing
Hexagon keyway
Bearing

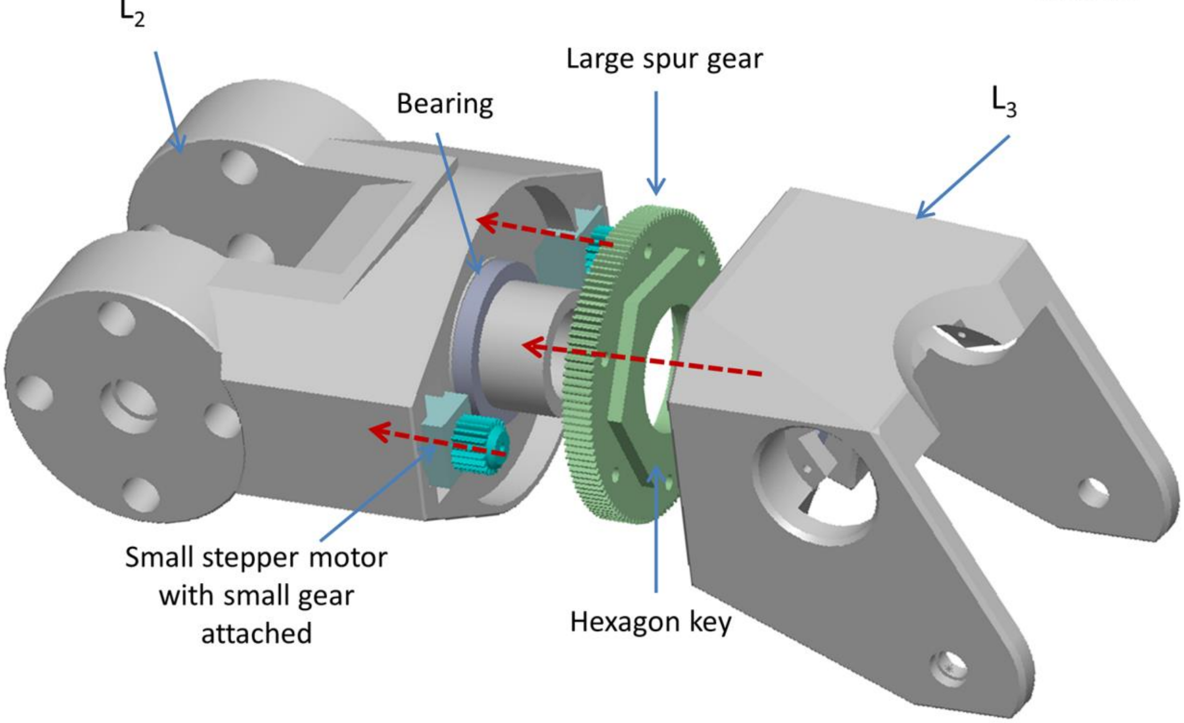
L$_2$
Large spur gear
Bearing
L$_3$
Small stepper motor with small gear attached
Hexagon key

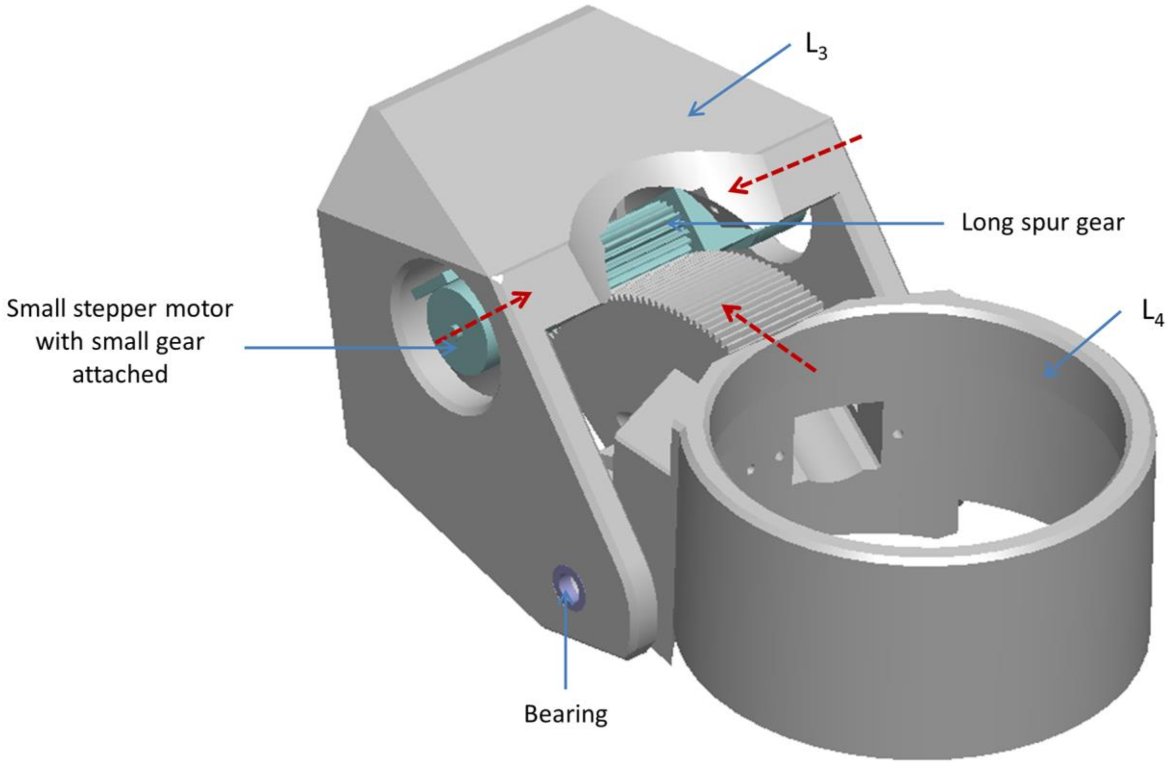
L$_3$
Long spur gear
Small stepper motor with small gear attached
L$_4$
Bearing

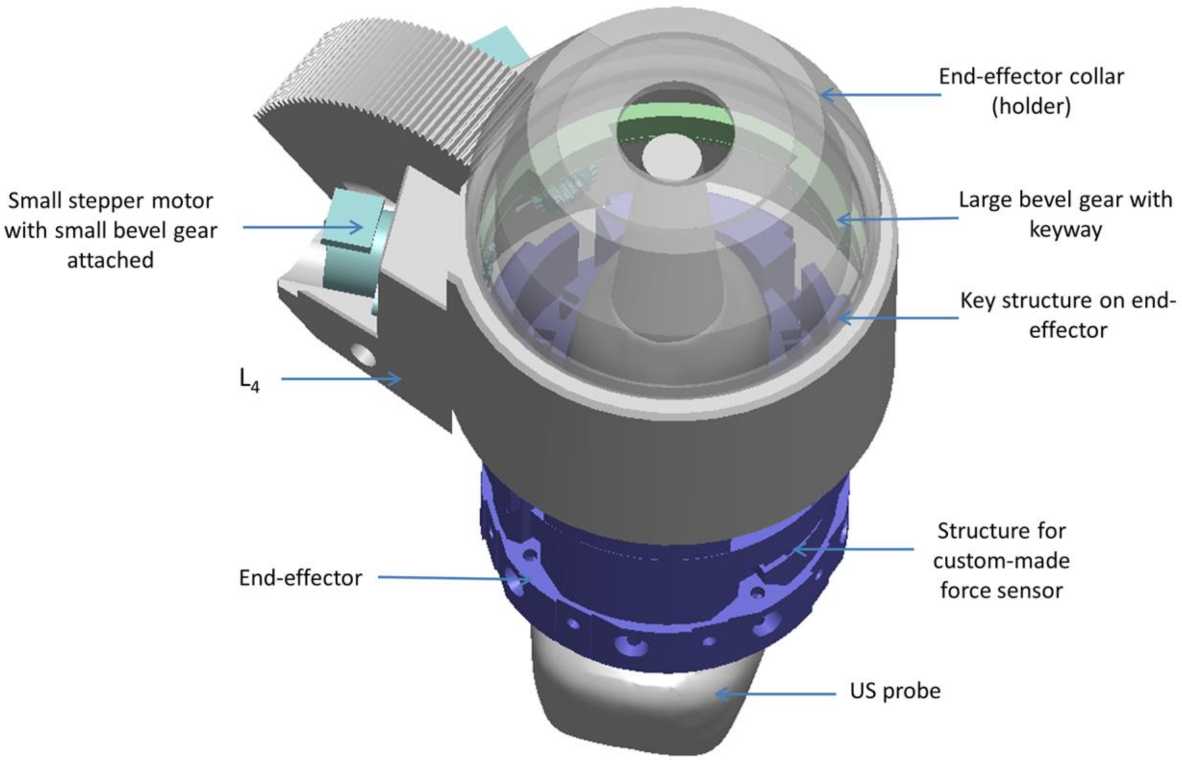
End-effector collar (holder)
Small stepper motor with small bevel gear attached
Large bevel gear with keyway
Key structure on end-effector
L$_4$
Structure for custom-made force sensor
End-effector
US probe

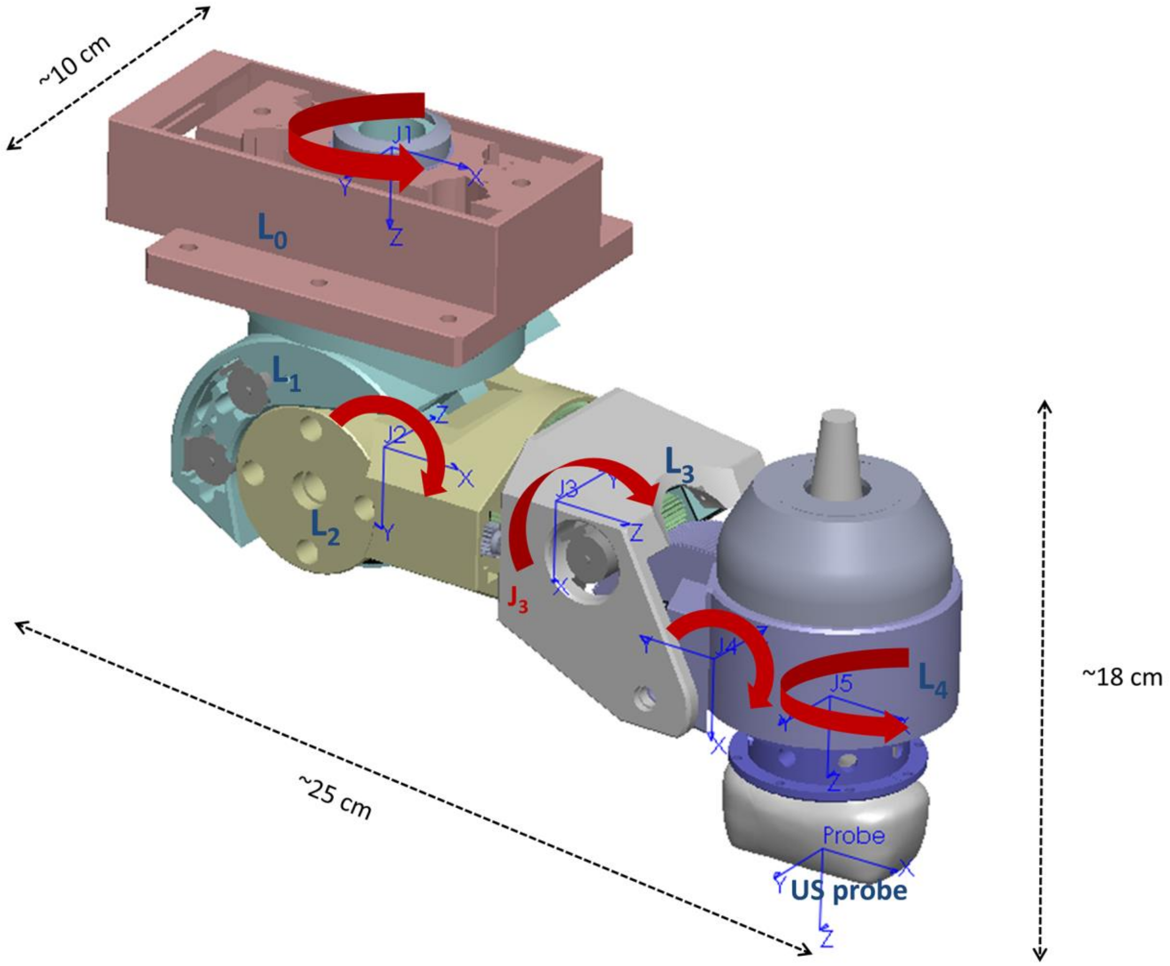
~10 cm
J1
Y
X
Z
L0
L1
J2
Z
X
Y
L2
L3
J3
Y
Z
X
J3
J4
Y
X
J5
Y
Z
L4
~18 cm
~25 cm
Probe
Y
X
US probe
Z

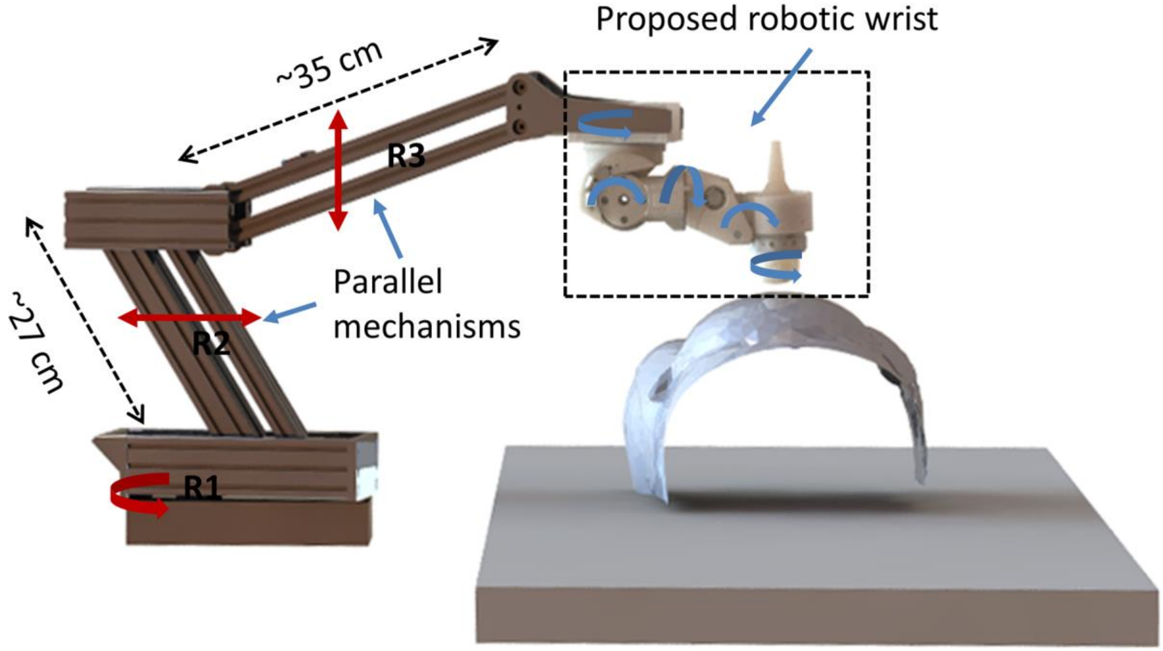
Proposed robotic wrist
~35 cm
R3
~27 cm
Parallel mechanisms
R2
R1

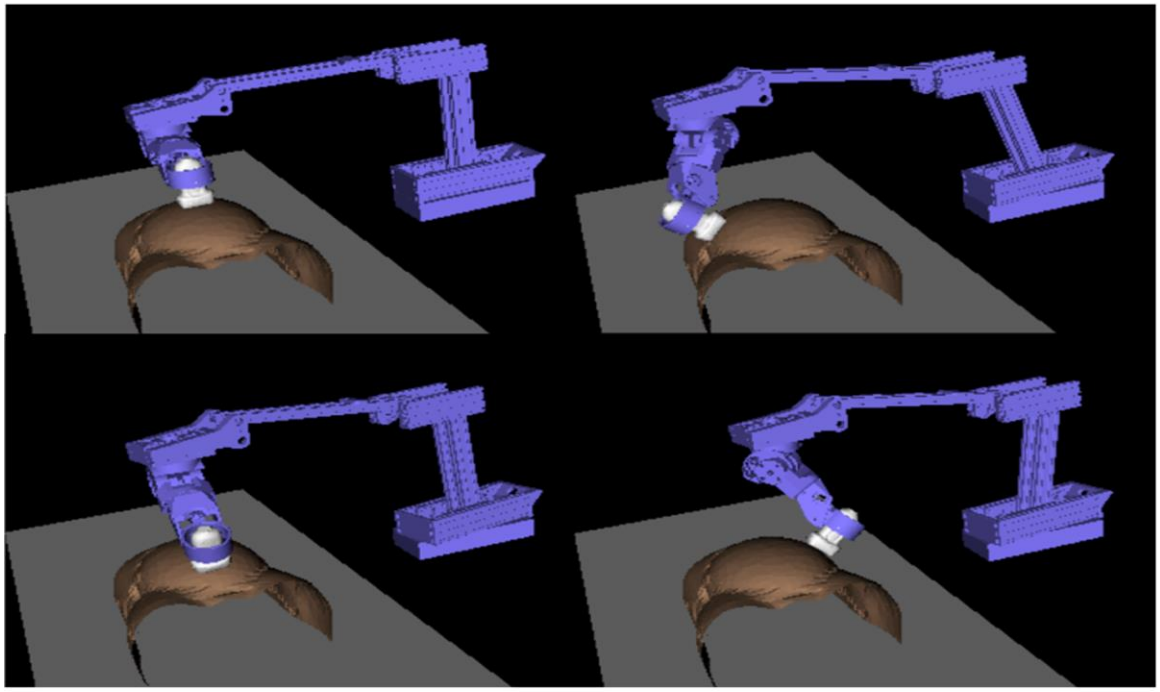

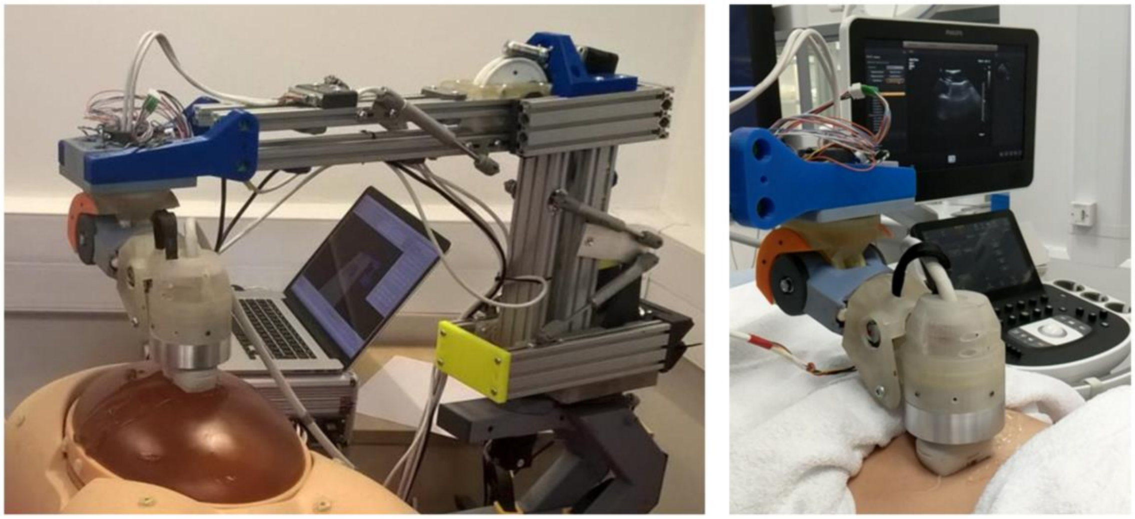

(a) (b)